

# Synchronous Fluorescence Spectrometric Methodology in the Wavelength Domain

Yao-Qun Li,<sup>1,2</sup> Xian-Zhi Huang,<sup>1</sup> and Jin-Gou Xu<sup>1</sup>

Received July 28, 1998; accepted January 29, 1999

---

Theoretical relationships suitable for both constant-wavelength and variable-angle synchronous fluorescence in the wavelength domain were obtained for the calculation of peak location, intensity, and half-width of synchronous fluorescence spectra. The calculated values were compared with experimental data and the data derived from the literature equations, indicating that the proposed methods are feasible, less formidable, and more straightforward in the wavelength domain than previous ones. The proposed approaches provide a theoretical guide for the experimental design of synchronous fluorescence spectrometric methods in the wavelength domain. On the basis of the theoretical derivation, special characteristics of the peak half-bandwidths of the spectra were revealed. In certain cases, the bandwidth of a variable-angle synchronous spectrum is of less practical meaning.

---

**KEY WORDS:** Spectrofluorimetry; synchronous fluorescence spectra; peak maximum; bandwidth; variable-angle synchronous scanning.

## INTRODUCTION

Synchronous fluorescence spectroscopy (SFS) has become a particularly active field [1] owing to its apparent advantages, e.g. a simplification in spectral complexity, an improvement in selectivity, and a decrease in scattering light interference. There are three variants of SFS, i.e., constant-wavelength [2–8], constant energy [9–11] (CE), and variable-angle [12–16] [VA; or variable-offset, (VO)] techniques, depending on the scanning mode of the spectra. CWSFS maintains a constant-wavelength difference,  $\Delta\lambda$ , while CESFS keeps a constant-energy difference,  $\Delta\nu$ , between the excitation and the emission monochromators during the scan. Both CW and CE scan modes correspond to a straight line with a slope of 1 across an excitation–emission matrix (EEM) with axes in nanometers and centimeters<sup>-1</sup>, respectively. VASFS implements different scan speeds for the excitation and emission monochroma-

tors, allowing the slope to vary from 1. The latter offers considerable flexibility and potentially improved performance compared to other scan modes. Cabaniss [17] distinguished between variable-angle scans with the slope defined in wavelength (VAW) and in energy (VAE). VAE scans have seldom been used yet.

The characteristics of all synchronous fluorescence spectra can be represented by three spectral parameters, i.e., the peak wavelength, peak intensity, and half-bandwidth. Theoretical investigations on the relationship of these parameters with corresponding excitation spectra, emission spectra, and scan parameters would facilitate the full realization of merits of SFS and subsequent scan parameter optimization. Literature reports [17–20] concerned with the theoretical processing of SFS have all assumed fluorescence excitation and emission peaks to be represented as Gaussian functions of frequency or reciprocal wavelength (wavenumbers). Hence, the calculations are straightforward for SFS methods in the frequency domain, including CESFS [18] and VAESFS [17], and exact relationships can be obtained. However, predicting synchronous spectra acquired in the wavelength

<sup>1</sup> SEDC Laboratory of Analytical Sciences, Department of Chemistry, Xiamen University, Xiamen 361005, P.R. China.

<sup>2</sup> To whom correspondence should be addressed.

domain including CWSFS and VAWSFS was less straightforward (based on the Gaussian assumption in frequency) and contained necessary approximations [19,17].

Our recent work has shown that theoretical calculations are feasible for CWSFS on the assumption that excitation and emission spectra are represented as the products of Gaussians in wavelength [21]. In this paper we develop synchronous fluorescence spectrometric methodology suitable for both CW and VAW modes. Expressions of the theoretical calculation for spectral parameters of SFS in the wavelength domain are given. The calculations are less formidable in the wavelength domain and exact relationships can be obtained. Consequently, special characteristic of the peak half-bandwidth of VASFS are revealed. Two half-bandwidth values exist for the same spectrum. To evaluate the properties of a VA spectrum, both bandwidths should be considered.

CWSFS has been applied widely in environmental and pharmaceutical analysis. A proper and direct theoretical calculation should reduce the trial-and-error test and speed up the establishment of the measurement approach. To date, VAWSFS is not yet commonly applied due to the difficulty of access, though the technique provides a higher flexibility and selectivity. The easily used theory of VAWSFS would reduce the fear of designing a suitable VAW synchronous scan path. Investigation of its special characteristics is particularly useful for the application of this technique.

## THEORY

Fluorescence excitation and emission peaks are represented as Gaussian functions of wavelength. Excitation intensity  $X(\lambda_i)$  at excitation wavelength  $\lambda_i$ , relative to maximum intensity  $X_0$  (arbitrary intensity units), can be represented as

$$X(\lambda_i) = X_0 \exp[-(\lambda_i - \lambda_{i0})^2/2\sigma_i^2] \quad (1)$$

where  $\lambda_{i0}$  is the wavelength position of the excitation peak maximum (nm) and  $\sigma_i$  the standard deviation of the excitation peak (nm). Similarly, emission intensity  $Y(\lambda_j)$  at emission wavelength  $\lambda_j$  (nm), relative to maximum intensity  $Y_0$ , can be represented as

$$Y(\lambda_j) = Y_0 \exp[-(\lambda_j - \lambda_{j0})^2/2\sigma_j^2] \quad (2)$$

where  $\lambda_j$  is the wavelength of emission peak maximum (nm) and  $\sigma_j$  is the standard deviation of the emission peak (nm). Hence, the fluorescence intensity  $M$  excited at  $\lambda_i$  and observed at  $\lambda_j$  is given by

$$M = M_0 \exp[-(\lambda_i - \lambda_{i0})^2/2\sigma_i^2 - (\lambda_j - \lambda_{j0})^2/2\sigma_j^2] \quad (3)$$

where  $M_0$  is the maximum intensity determined by sample and instrumental conditions. Under usual conditions, we can obtain  $M_0 = Y_0 = X_0$ , because each is the same detector response to the same fluorescence excited at  $\lambda_{i0}$  and monitored at  $\lambda_{j0}$ .

For VAWSFS, the wavelength interval between the excitation and the emission monochromators changes linearly with time. To determine a scan path for VAWSFS, more than one variable is needed, while a CW or CE scan needs only a variable  $\Delta\lambda$  or  $\Delta\nu$ . Based on the principle of the VAW scan, the following equation can be obtained:

$$\lambda_j = \beta(\lambda_i - \lambda_i^*) + \lambda_j^* \quad (4)$$

where  $\beta$  is the ratio of the scan speed for the emission monochromator to that for the excitation monochromator or the slope of the VAW path across an EEM, and  $\lambda_i^*$  and  $\lambda_j^*$  are the initial wavelength positions for excitation and emission monochromators, respectively.

Substitution of Eq. (4) into Eq. (3) gives

$$M = M_0 \exp[-(\lambda_i - \lambda_{i0})^2/2\sigma_i^2 - (\beta\lambda_i - \beta\lambda_i^* + \lambda_j^* - \lambda_{j0})^2/2\sigma_j^2] \quad (5)$$

Here  $M_0$  is a constant value for a defined sample and instrument. The relative fluorescence intensity for VAW scans can be expressed as

$$I_s = \exp[-(\lambda_i - \lambda_{i0})^2/2\sigma_i^2 - (\beta\lambda_i - \beta\lambda_i^* + \lambda_j^* - \lambda_{j0})^2/2\sigma_j^2] \quad (6)$$

where  $I_s$  varies between 0 and 1 relative to  $M_0$ .

Inman *et al.* [18] took the derivative of the CESF intensity to find the location of the maximum intensity and found the half-bandwidth of the CESF spectra by algebraic substitution. A similar method can be used for VAWSF spectra. The three spectral parameters were then derived as follows (see the Appendix for the derivation procedure). For the locations of the intensity maximum of VAWSFS  $\lambda_{is0}$  in terms of the excitation wavelength, we have

$$\lambda_{is0} = [W_i^2\beta(\lambda_i^*\beta + \lambda_{j0} - \lambda_j^*) + W_j^2\lambda_{i0}]/(W_i^2\beta^2 + W_j^2) \quad (7)$$

For the relative intensity of the VAW maximum  $I_{s0}$ , we have

$$I_{s0} = \exp[-(4 \ln 2)(\lambda_i^*\beta + \lambda_{j0} - \lambda_j^* - \beta\lambda_{i0})^2/(W_i^2\beta^2 + W_j^2)] \quad (8)$$

For the half-bandwidth  $W_{is}$ , we have

$$W_{is} = W_i W_j / (W_i^2 \beta^2 + W_j^2)^{1/2} \quad (9)$$

The theoretical calculations of the intensity, wavelength position, and half-bandwidth of VAWSFS in terms of excitation wavelength are then given by Eqs. (8), (7), and (9), respectively.

Since VAWSF spectra combine the excitation and emission information, the spectral parameters can also be expressed in terms of the emission wavelength. We have

$$\lambda_{js0} = \beta(\lambda_{is0} - \lambda_i^*) + \lambda_j^* = [W_j^2(\lambda_{i0}\beta + \lambda_j^* - \beta\lambda_i^*) + \beta^2 W_i^2 \lambda_{j0}] / (W_i^2 \beta^2 + W_j^2) \quad (10)$$

The two positions  $\lambda_{jh1}$  and  $\lambda_{jh2}$  corresponding to half the peak intensity in terms of emission wavelength are related to the two positions  $\lambda_{ih1}$  and  $\lambda_{ih2}$  corresponding to half the peak intensity in terms of excitation wavelength by Eq. (1). Hence, there is

$$\lambda_{jh2} - \lambda_{jh1} = [\beta(\lambda_{ih2} - \lambda_i^*) + \lambda_j^*] - [\beta(\lambda_{ih1} - \lambda_i^*) + \lambda_j^*] = \beta(\lambda_{ih2} - \lambda_{ih1}) \quad (11)$$

With the definition of half-bandwidth,  $W = |\lambda_{h2} - \lambda_{h1}|$ , the half-bandwidth of VAWSF peak in terms of the emission wavelength can be obtained by

$$W_{js} = \beta W_{is} \quad \text{or} \quad W_i W_j / (W_i^2 + W_j^2 \beta^{-2})^{1/2} \quad (12)$$

Concerning the intensity of the VAWSF peak, there is no difference in expression in terms of excitation or emission wavelength.

## EXPERIMENTAL

The fluorescence spectra were recorded with a laboratory-constructed microcomputer-controlled versatile spectrofluorimeter, equipped with a 500-W xenon lamp and excitation and emission grating monochromators. This apparatus can be used for measurements of fluorescence excitation spectra, emission spectra, and all kinds of synchronous spectra (including CW, CE, and VA) as well as their derivative spectra [11,14–16].

1-Naphthol and 2-naphthol were commercially available with a purity of more than 99%. Phenol, 2,2'-dihydroxybiphenyl, and 4-hydroxybiphenyl were all analytical reagent grade in purity. 1-Naphthol and 2-naphthol stock solutions were prepared, respectively, in an aqueous medium (0.1 M KOH) and stored in the dark. Phenol solutions were prepared in water. 2,2'-Dihydroxybiphenyl and 4-hydroxybiphenyl solutions were prepared in

0.01 N HCl. Doubly deionized water was used throughout.

## RESULTS AND DISCUSSION

### CWSFS

CWSFS is, basically, VAWSFS in a particular case, i.e.,  $\beta = 1$ , and we have

$$\Delta\lambda = \lambda_j^* - \lambda_i^* \quad (13)$$

Therefore, the following can be obtained from Eqs. (7), (8), and (9):

$$\lambda_{is0} = [W_i^2(\lambda_{j0} - \Delta\lambda) + W_j^2 \lambda_{i0}] / (W_i^2 + W_j^2) \quad (14)$$

$$I_{s0} = \exp[-(4\ln 2)(\lambda_{j0} - \lambda_{i0} - \Delta\lambda)^2] / (W_i^2 + W_j^2) \quad (15)$$

$$W_s = W_i W_j / (W_i^2 + W_j^2)^{1/2} \quad (16)$$

where  $W_{is}$  is replaced by  $W_s$  since the half-bandwidth in terms of the excitation wavelength is equal to that in terms of the emission wavelength in CWSF spectra. Then these expressions become the same as those derived directly from the CWSF principle [21].

### Bandwidths

Two empirical relationships for the half-bandwidth of CW synchronous peaks were reported in Refs. 19 and 20. The three kinds of calculated peak half-bandwidths derived from the proposed Eq. (16) and the two empirical equations have been compared with experimental data for the CW synchronous fluorescence spectra of nine compounds [21,22]. The average error was  $+0.03 \pm 1.6$  (SD) with the proposed Eq. (16),  $+0.4 \pm 2.8$  with the empirical equation in Ref. 19, and  $-4.4 \pm 2.2$  with the empirical equation in Ref. 20. The proposed Eq. (16) provides apparently more accurate bandwidths of CW synchronous spectra than the reported empirical relationships. In fact, the bandwidth results coincide with the approach of Cabaniss [17] and indicate that the Gaussian distribution of intensity versus wavelength is feasible and more straightforward.

### Peak Intensity and Position

The calculated values were compared with experimental data for peak positions and intensities of CW synchronous fluorescence spectra for 1-naphthol and 2-naphthol with a variety of  $\Delta\lambda$  values (66, 100, 126, 160,

**Table I.** Comparison of Predicted Values of the Peak Positions of Some Polynuclear Hydrocarbons

	Lit. $\lambda_{jso}$ (nm)		Prop. $\lambda_{jso}$ (nm)	
	$\Delta\lambda$ 19 nm	$\Delta\lambda$ 1.5 nm	$\Delta\lambda$ 19 nm	$\Delta\lambda$ 1.5 nm
Benzo(k)fluoranthene	403, 425	403	403, 425	403
Benzo[ $\alpha$ ]pyrene	403, none	403	None	
Perylene	433, 441	438	435, 443	437
Anthanthrene	429, 437, 449	430	429, <sup>a</sup> —, <sup>a</sup> 449	430

<sup>a</sup> No emission peak half-width was given in Ref. 19.

and 180 nm) [21]. In general, better results were obtained from the proposed method.

Lloyd and Evett [19] predicted values of  $\lambda_{jso}$  for some polynuclear hydrocarbons (see Table V in Ref. 19). The proposed method is used to calculate  $\lambda_{jso}$  for these compounds. In comparison with the experimental data (Fig. 2 in Ref. 19), the proposed method and the reference's method give results in good agreement as shown in Table I, and obviously our method is more straightforward.

### VAWSFS

The proposed expressions were used to predict the spectral parameters of VAWSFS. Comparisons with experimental results are given using phenol, 2,2'-dihydroxybiphenyl, and 4-hydroxybiphenyl as model compounds.

The fluorescence excitation spectra were obtained at the emission peak position, and vice versa, emission spectra at the excitation peak position. The half-bandwidths and peak positions of the fluorescence excitation and emission spectra for these three compounds are given in Table II.

The spectral parameters calculated with the proposed expressions and those measured from the observed VA synchronous fluorescence spectra with various VAW scan paths are given in Tables III, IV, and V for phenol, 4-hydroxybiphenyl, and 2,2'-dihydroxybiphenyl, respectively. Since the calculated data of peak intensities of VASF spectra are expressed by ratios of 0–1, the experimental synchronous fluorescence peak intensity is defined as the ratio of the observed synchronous peak

height to the average of the observed excitation and emission peak heights (under maximum emission and maximum excitation, respectively). Though there is no literature data for comparison, Tables III–V show that the proposed theoretically calculated data coincide with the experimental results. Therefore, such a theoretical calculation can be used to predict the VAW synchronous spectra and make the design of the best VAW scan path simpler and easier without resorting to tedious experimental trials. The following is an application of the proposed synchronous fluorescence theory, which we would like to emphasize.

It is well known that in conventional spectra, a bandwidth corresponds to a spectral peak. It is rather vague, however, simply to give a value of a peak half-bandwidth of VA synchronous spectra without indicating whether it is in terms of excitation or emission wavelength. Two parameters are needed to illustrate the peak bandwidth of a VA synchronous scan, i.e., the peak half-bandwidth  $W_{is}$  in terms of excitation wavelength (or frequency) and  $W_{ie}$  in terms of emission wavelength (or frequency).

There are three cases for relative values of  $W_i$  and  $W_j$ :

- (1)  $W_i = W_j$
- (2)  $W_i \gg W_j$
- (3)  $W_i \ll W_j$

Case 1:  $W_i = W_j$

Equations (9) and (12) can be reduced to

$$W_{is} = W_i/(\beta^2 + 1)^{1/2}, \quad W_{js} = W_j/(\beta^{-2} + 1)^{1/2} \quad (17)$$

The scan speed ratio of emission to excitation,  $\beta$ , is a key scan parameter. When  $\beta$  becomes larger,  $W_{is}$  will decrease, while  $W_{js}$  will increase. The opposite is true when  $\beta$  decreases:  $W_{is}$  will increase, while  $W_{js}$  will decrease. Figure 1 gives an example with a model compound possessing  $W_i = W_j = 30$  nm. As shown in the figure, in such a case, there is no particular meaning for the bandwidth of the VAW synchronous spectra because

**Table II.** Fluorescence Characteristics of Three Compounds

Compound	$\lambda_i$ (nm)	$\lambda_j$ (nm)	$W_i$ (nm)	$W_j$ (nm)
Phenol	274	300	18.6	35
2,2'-Dihydroxybiphenyl	285	394	24	65
4-Hydroxybiphenyl	276	335	44	47

**Table III.** Comparison of Calculated Data of Spectral Parameters with Experimental Results for Phenol

	No.						Mean	SD
	1	2	3	4	5	6		
Scan parameter								
$x$ (nm/min) <sup>a</sup>	120	120	120	120	120	60		
$y$ (nm/min) <sup>b</sup>	60	90	150	180	240	180		
$\lambda_i^*$ (nm)	220	220	240	240	240	260		
$\lambda_j^*$ (nm)	260	260	260	260	250	260		
$\lambda_{iso}$ (nm)								
Exptl.	278.0	274.0	274.0	271.0	269.0	276.0		
Calcd.	275.7	273.9	273.4	271.2	269.2	275.9		
Error	-2.3	-0.1	0.6	+0.2	+0.2	-0.1	-0.5	1.0
$I_{s0}$								
Exptl.	0.759	0.983	1.000	0.862	0.724	1.017		
Calcd.	0.700	1.000	0.990	0.846	0.709	0.960		
Error	-0.041	+0.017	-0.010	-0.016	-0.015	-0.057	-0.020	0.026
$W_{is}$ (nm)								
Exptl.	14.5	17.5	15.5	17.0	15.0	8.5		
Calcd.	18.0	17.3	15.5	14.5	12.7	9.9		
Error	+3.5	-0.2	0.0	-2.5	-2.3	+1.4	0.0	2.3

<sup>a</sup> Scan speed of the excitation monochromator.<sup>b</sup> Scan speed of the emission monochromator.

the half-bandwidth value decrease, while the other increases for the same spectrum. Therefore, when designing an experimental procedure for a multicomponent analysis, we do not need to pay much attention to the bandwidth of the spectra. The selection of the scan parameter  $\beta$  should be based mainly on the separation of VAW peak positions to avoid mutual spectral interference.

Case 2:  $W_i \gg W_j$

The bandwidth of VAWSF spectra is determined mainly by  $W_j$  and  $\beta$ , based on Eqs. (9) and (12).

$$W_{is} \cong W_j/\beta, \quad W_{js} \cong W_j \quad (18)$$

$W_{is}$  decreases and  $W_{js}$  maintains almost a fixed value with

**Table IV.** Comparison of Calculated Data of Spectral Parameters with Experimental Results for 4-Hydroxybiphenyl

	No.						Mean	SD
	1	2	3	4	5	6		
Scan parameter								
$x$ (nm/min) <sup>a</sup>	120	120	120	80	150	240		
$y$ (nm/min) <sup>b</sup>	100	150	200	120	120	120		
$\lambda_i^*$ (nm)	220	220	220	220	220	220		
$\lambda_j^*$ (nm)	270	270	270	290	290	290		
$\lambda_{iso}$ (nm)								
Exptl.	287.0	273.3	261.0	262.0	274.7	285.0		
Calcd.	284.3	273.7	263.9	258.7	276.1	282.1		
Error	-2.7	+0.4	+2.9	-3.3	+1.4	-2.9	-0.7	2.6
$I_{s0}$								
Exptl.	0.778	0.971	0.833	0.628	1.006	0.689		
Calcd.	0.769	0.987	0.746	0.526	1.000	0.743		
Error	-0.009	+0.016	-0.087	-0.102	-0.006	+0.054	-0.022	0.060
$W_{is}$ (nm)								
Exptl.	26.6	31.2	28.0	30.0	36.8	34.0		
Calcd.	34.7	28.6	23.7	25.5	35.2	39.9		
Error	+8.1	-2.6	-4.3	-4.5	-1.6	+5.9	+0.2	5.4

<sup>a</sup> Scan speed of the excitation monochromator.<sup>b</sup> Scan speed of the emission monochromator.

**Table V.** Comparison of Calculated Data of Spectral Parameters with Experimental Results for 2,2'-Dihydroxybiphenyl

	No.						Mean	SD
	1	2	3	4	5	6		
Scan parameter								
$x$ (nm/min) <sup>a</sup>	120	120	120	200	200	200		
$y$ (nm/min) <sup>b</sup>	180	160	150	180	120	60		
$\lambda_i^*$ (nm)	220	220	220	240	240	240		
$\lambda_j^*$ (nm)	320	320	320	360	360	360		
$\lambda_{is0}$ (nm)								
Exptl.	281.0	283.0	285.0	284.0	285.0	283.3		
Calcd.	281.3	285.1	284.0	284.3	285.5	285.8		
Error	+0.3	+2.1	-1.0	+0.3	+0.5	+2.5	+0.8	1.3
$I_{is0}$								
Exptl.	0.752	0.995	0.971	0.982	0.899	0.613		
Calcd.	0.758	1.000	0.972	0.975	0.970	0.762		
Error	+0.006	+0.005	+0.001	-0.007	+0.071	+0.149	+0.038	0.062
$W_{is}$ (nm)								
Exptl.	24.0	21.2	22.6	24.0	24.0	23.7		
Calcd.	21.0	21.5	21.8	22.8	23.4	23.9		
Error	-3.0	+0.3	-0.8	-1.2	-0.6	+0.2	-0.8	1.2

<sup>a</sup> Scan speed of the excitation monochromator.

<sup>b</sup> Scan speed of the emission monochromator.

an increase in  $\beta$ . Hence, the increase in  $\beta$  could narrow the bandwidth of the VAWSF spectra.

### Case 3: $W_i \ll W_j$

The bandwidth of VAWSFS is determined mainly by  $W_i$  and  $\beta$ .

$$W_{is} \cong W_i, \quad W_{js} \cong \beta W_i \quad (19)$$

The decrease in  $\beta$  narrows the bandwidth of VAWSF spectra. Usually, we use  $W_{js}$  as a parameter to describe the bandwidth of synchronous spectra. For CESF spectra, that is enough. In VASF spectra,  $W_{is}$  should also be clarified. A major distinction of VASFS from CW or CE synchronous fluorescence is its bandwidth expression. For experimental design,  $\beta$  is a key scan parameter and it is necessary to take it into careful consideration.

## CONCLUSIONS

This paper discusses the synchronous fluorescence spectrometric methodology in the wavelength domain. The proposed calculations, which are feasible and straightforward, provide a guideline for the experimental design of synchronous fluorescence spectrometric methods in the wavelength domain. It has been pointed out

that the bandwidth of a variable-angle synchronous spectrum is of less practical meaning when the bandwidths of excitation and emission spectra are similar. Comparisons among the proposed methods, literature methods, and experimental data have been made. The predictions provide a guideline for the experimental design to relieve the trial-and-error test and facilitate the establishment of measurement procedures. The proposed approach is useful for the applications of synchronous fluorescence spectrometry, especially variable-angle synchronous fluorescence which is less common due to the difficulty in selecting suitable scan parameters.

## ACKNOWLEDGMENTS

This research was supported by the National Natural Science Foundation of China. We thank Guo-Zhen Chen for his helpful comments.

## APPENDIX

In order to obtain peak locations, the VAWSFS intensity function is differentiated with respect to the excitation wavelength and set equal to zero. Therefore, the location

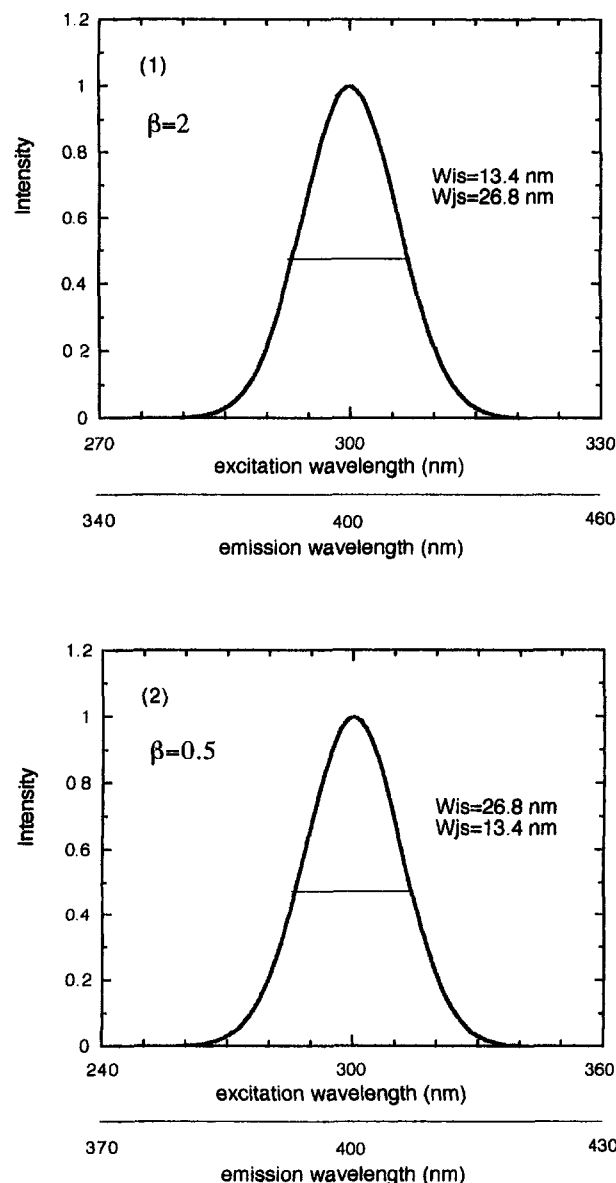


Fig. 1. VAW synchronous fluorescence spectra for a model compound with half-bandwidths of 30 nm for both excitation and emission spectra. (1)  $\beta = 2$ . (2)  $\beta = 0.5$ .

of the intensity maximum of VAW scan  $\lambda_{is0}$  in terms of the excitation wavelength can be derived as follows:

$$\lambda_{is0} = [\sigma_i^2 \beta (\lambda_i^* \beta + \lambda_{j0} - \lambda_j^*) + \sigma_j^2 \lambda_{i0}] / (\sigma_i^2 \beta^2 + \sigma_j^2) \quad (A1)$$

Because the half-bandwidth  $W$  (nm), by definition, is related to  $\sigma$  by

$$W = (8 \ln 2)^{1/2} \sigma \quad (A2)$$

Eq. (7) can be deduced by the substitution of Eq. (A2) into Eq. (A1). Eq. (8) can then be deduced by combining Eqs. (6), (7), and (A2), followed by simplification.

The half-bandwidth of the synchronous fluorescence peak  $W_{is}$  can be determined from the difference between the two positions  $\lambda_{ih1}$  and  $\lambda_{ih2}$  corresponding to half the peak intensity  $I_{s0}$ . The use of Eq. (6) results in

$$\exp [-(\lambda_{ih} - \lambda_{i0})^2 / 2\sigma_i^2 - (\beta\lambda_{ih} - \beta\lambda_i^* + \lambda_j^* - \lambda_{j0})^2 / 2\sigma_j^2] = 0.5I_{s0} \quad (A3)$$

Substituting Eqs. (8) and (A2) into Eq. (A3) and solving Eq. (A3) gives  $\lambda_{ih1}$  and  $\lambda_{ih2}$  and the difference between them is equal to the half-bandwidth. Hence, the half-bandwidth of VAWSFS can be deduced as Eq. (9).

## REFERENCES

1. S. A. Soper, L. B. McGown, and I. M. Warner (1994) *Anal. Chem.* **66**, 428R–444R.
2. P. Canizares and M. D. Luque de Castro (1996) *Fresenius J. Anal. Chem.* **354**, 291–295.
3. T. A. Taylor and H. H. Patterson (1987) *Anal. Chem.* **59**, 2180–2187.
4. T. Vo-Dinh (1978) *Anal. Chem.* **50**, 396–401.
5. T. P. Ruiz, C. Martinez-Lozano, V. Tomas, and J. Carpena (1998) *Talanta* **45**, 969–976.
6. A. Seritti, L. Nannicini, and R. D. Vecchio (1996) *Environ. Tech.* **17**, 25–33.
7. J. A. M. Pulgarin, A. A. Molina, and P. F. Lopez (1997) *Anal. Biochem.* **245**, 8–16.
8. W. C. Bell, K. S. Booksh, and M. L. Myrick (1998) *Anal. Chem.* **70**, 332–339.
9. E. L. Inman and J. D. Winefordner (1982) *Anal. Chem.* **54**, 2018–2022.
10. J. J. B. Nevado, J. A. M. Pulgarin, and M. A. G. Laguna (1995) *Talanta* **42**, 129–136.
11. Y. Q. Li, X. Z. Huang, J. G. Xu, and G. Z. Chen (1992) *Anal. Chim. Acta* **256**, 285–291.
12. J. A. M. Pulgarin and A. A. Molina (1996) *Anal. Chim. Acta* **319**, 361–368.
13. A. S. Carretero, C. C. Blanco, and A. F. Gutierrez (1997) *Anal. Chim. Acta* **353**, 337–344.
14. Y. Q. Li and L. Shi (1995) *Chin. Chem. Lett.* **6**, 789–790.
15. Y. Q. Li, X. Z. Huang, J. G. Xu, and G. Z. Chen (1994) *Talanta* **41**, 695–701.
16. Y. Q. Li and X. Z. Huang (1997) *Fresenius J. Anal. Chem.* **357**, 1072–1075.
17. S. E. Cabaniss (1991) *Anal. Chem.* **63**, 1323–1327.
18. E. L. Inman, L. A. Files, and J. D. Winefordner (1986) *Anal. Chem.* **58**, 2156–2160.
19. J. B. F. Lloyd and I. W. Evett (1977) *Anal. Chem.* **49**, 1710–1715.
20. Ph. Baudot and J. C. Andre (1982) *Anal. Lett.* **15**, 471–492.
21. Y. Q. Li, X. Z. Huang, and J. G. Xu (1993) *Fenxi Huaxue* **21**, 770–774.
22. J. G. Xu and R. T. Xu (1990) *Chem. J. Chin. Univ.* **11**, 350–354.